Rubidium-doped epitaxial C_{60} thin films: synthesis and electronic transport

1993 J. Phys.: Condens. Matter 5 L409

(http://iopscience.iop.org/0953-8984/5/33/006)

J. Phys.: Condens. Matter 5 (1993) L409–L414. Printed in the UK

LETTER TO THE EDITOR

Rubidium-doped epitaxial C_{60} thin films: synthesis and electronic transport

W B Zhao†, X D Zhang†, J Chen†, J Tan†, K Wu†, J L Zhang†, C Y Li†, D L Yin†, Z N Gu‡, X H Zhou‡ and Z X Jin‡

† Department of Physics, Peking University, Beijing 100871, People's Republic of China
‡ Department of Chemistry, Peking University, Beijing 100871, People's Republic of China

Received 22 June 1993

Abstract. Epitaxial thin films of C_{60} have been synthesized and doped with rubidium. Above 80 K, the sample resistivity shows classic metallic temperature dependence just like that of K_3C_{60} single crystals. However, the temperature coefficient changes sign at about 80 K, and the resistivity increases by 5% before the superconducting state near 30 K is reached. As for different samples, the zero-resistance temperature varies sharply with the sample lowest resistivity and can be fitted to a functional form of $T_{c0} = a + b\rho^{-5}$. The critical current density J_c is 10^3–10^4 A cm^{-2} at $\simeq$ 5 K, 0 T and it is found that J_c is proportional to $(1 - T/T_c)^{\alpha}$, where α is in the range 1.3–2.0. Furthermore, the voltage–current characteristic of the films is very similar to that of high-T_c superconductors and remains a problem for further research on this new kind of material.

The occurrence of conductivity in alkali fulleride compounds [1] and superconductivity at relatively high temperatures in A_3C_{60} (A = K, Rb, Cs or a mixture of these) [2–5] has stimulated many investigations of both the normal and superconducting properties, but little work on transport in these materials, especially for Rb_3C_{60} specimens. Rosseinsky *et al* [3] tried to dope Rb into polycrystal C_{60} thin films; however, the resistance measurements showed that the sheet resistance increased rapidly on cooling the sample to liquid-nitrogen temperature, and no zero resistance was found down to 5 K. Later, Ogata *et al* [6] successfully observed a superconducting transition in Rb_xC_{60} thin films, but the temperature coefficient of the resistance (TCR) was negative in the normal state and the zero-resistance temperature (2.5 K) was far lower than T_c (28 K) measured by the magnetic method in bulk samples [3]. As for K-doped C_{60} specimens, both sizable K_3C_{60} single crystals [7] and epitaxial thin films [8] have been synthesized with a very narrow superconducting transition width (0.2–0.7 K, 10–90%) and T_c similar to the magnetic measured value.

In this letter, we report the preparation details and preliminary results on electronic transport properties of epitaxial C_{60} thin films doped with Rb. From room temperature to ~80 K, the sample has a positive TCR and it can be fitted to a functional form of $\rho(T) = a + bT^2$, just like that of K_3C_{60} single crystals [7]. However, the TCR changes sign at ~80 K and the resistance increases by ~5% before reaching the superconducting state near 30 K. The transition width (~4 K) is relatively large and the critical current density J_c (10^3–10^4 A cm^{-2}) is not very high compared to that of K_3C_{60} [7, 8]. We believe that the high density of intrinsic stacking faults in the precursor C_{60} thin films, and hence the low diffusion rate, make it much more difficult to obtain high-quality Rb_3C_{60} specimens free from inhomogeneity and weak coupling between superconducting phases.

0953-8984/93/330409+06$07.50

The C_{60} was produced by the conventional AC arc method and purified by repeated liquid chromatography. The epitaxial thin films of C_{60} were grown by thermal evaporation of pure C_{60} (better than 99.8%) onto a freshly cleaved (001) mica substrate of 1 cm × 0.5 cm in a Balzers UMS-500 UHV system at a pressure of 1×10^{-7} Pa and substrate temperature of 200 °C. The deposition rate (~1 nm min^{-1}) and film thickness were monitored *in situ* by a quartz-crystal oscillator. The final film thickness (~200 nm) was again calibrated *ex situ* by a high-accuracy surface profilograph. The orientational ordering and the nature of the defects presented in the films were assessed by transmission electron diffraction and electron microscopy. The TEM study showed that the films were (111) epitaxed on the (001) mica cleaved plane; the fundamental structure of the C_{60} crystal is face-centred cubic with a lattice parameter of 1.42 nm; stacking faults are the main type of defect [8–10]. Very recently, Fisher *et al* [12] studied the overall quality of C_{60} thin films prepared by a similar method on mica, using both reflection-geometry and grazing-incidence-geometry x-ray scattering. Although they find that there is a 0.9° distribution of crystallite orientations in the film's plane (that is, the epitaxy is not perfect), the 45 nm in-plane correlation length is much larger than the Pippard length of 15 nm in K_3C_{60} [11], indicating that when the films are doped they should demonstrate intrinsic superconducting properties, which is consistent with our previous work on K-intercalated C_{60} films [8].

Prior to evaporation, four contacts for four-probe measurements were made by evaporating Ag, and connecting Cu wires with Ag paste. The Rb doping process was performed in a quartz tube by oil bath at a dynamic pressure of 5×10^{-4} Pa, where the alkali metals were placed at the bottom of the tube and the C_{60} thin film about 30 cm from the metal. To ensure adequate diffusion of the alkali metal into the C_{60} thin films, a very low doping rate was employed by adjusting the bath temperature. The doping process usually lasted for 10–20 h before the resistivity reached the equilibrium state.

For electrical transport measurements, the quartz tube was injected with a partial pressure of He after the doping process. The sample resistance was measured by Datron 1071 Autocal digital multimeter using a DC current ranging from 1 μA to 100 μA. The temperature was monitored by an Rh–Fe thermometer. Measurements for transport critical currents were performed by continuous DC currents with a criterion of 1 μA cm^{-1}.

Figure 1 shows the temperature dependence of the electrical resistivity of one of our best samples. The inset shows an expanded scale of the superconducting transition between 20 and 40 K. The resistivity of the sample near room temperature is about 10 mΩ cm. With decreasing temperature, the resistivity falls to a minimum of about 7.6 mΩ cm; however, the TCR changes sign at ~80 K and the resistivity increases by 5% before reaching the superconducting state near 30 K. As demonstrated by figure 2, the temperature dependence of the normal-state resistivity above 80 K can be fitted to a functional form of $\rho(T) = a + bT^{\alpha}$, with $\alpha = 2.13$, which is very similar to the intrinsic temperature dependence of the resistivity of K_3C_{60} single crystals [13]. Below 80 K, $\rho(T)$ displays a weak logarithmic dependence on temperature which can be seen from the inset of figure 2.

The weak coupling between the superconducting Rb_3C_{60} phases resulted in a broad transition with (10–90%) of 4.1 K, and zero-resistance temperature T_{c0} of 25.0 K. For different samples, we find that T_{c0} varies sharply with the sample lowest resistivity ρ(80 K), where $T_{c0}(\rho)$ can be fitted with the empirical formula $T_{c0} = a + b\rho^{-4.7}$ (see figure 3).

Both TEM [9, 10] and x-ray-diffraction [12] study have shown that the typical ordered stacking length of C_{60} in the epitaxial thin films is several tens of nanometres, and that the intrinsic stacking faults (HCP stacking) are the main type of defect which occur randomly in one of the four {111} planes. Considering the small superconducting coherence length (2.0 nm) [14], these stacking faults are crucial to the values of 'phase-locking' temperature

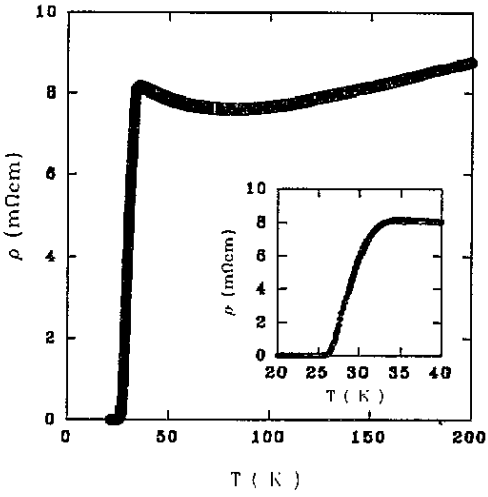

Figure 1. Temperature dependence of the resistivity of an Rb_3C_{60} thin film. The inset shows an expanded scale of the superconducting transition between 20 and 40 K.

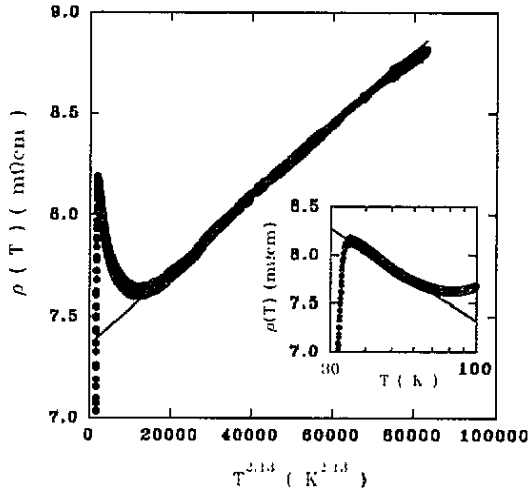

Figure 2. Plot of the normal-state resistivity $\rho(T)$ versus $T^{2.13}$ curve. We can see the linear relation of $\rho(T)$ to $T^{2.13}$ when T is higher than 80 K. The inset shows the weak logarithmic temperature dependence of sample resistivity before the superconducting transition.

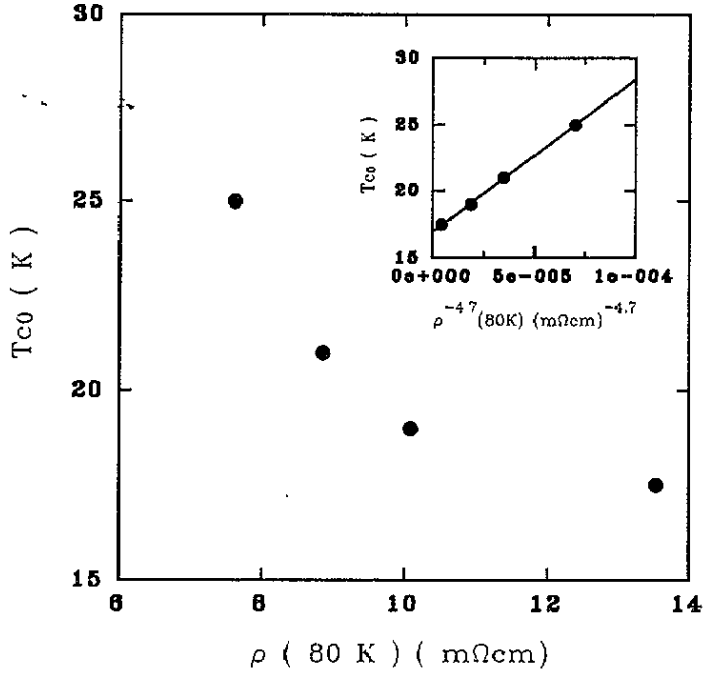

Figure 3. Plot of the sharp dependence of T_{c0} on the sample lowest resistivity ρ(80 K). From the inset curve, we can see the linear relation of T_{c0} to $\rho^{-4.7}$.

T_{c0}. Furthermore, because the energy differences between various phases of Rb_xC_{60} are not

large, of the order of 0.1 eV [15], it is plausible that there are mixed compositions around the stacking faults where strains are large and disorder is more important, thus promoting weak coupling between the superconducting phases. For these weakly coupled systems, the Josephson coupling energy E_J and Coulomb charging energy E_C are the two dominating parameters determining T_c. In [16], Imry *et al* have given the following equations:

$$kT_c/ZE_J = 2/\alpha|\ln\tfrac{3}{8}(\alpha - 1)| \qquad \text{for } \alpha \to 1$$

$$kT_c = ZE_J \qquad \text{for } \alpha \to \infty$$

where $\alpha = ZE_J/E_C$, $E_C = e^2/2C$ (C is the effective intergrain capacitance), and $E_J(T) = E_J(0)[\Delta(T)/\Delta(0)]\tanh[\Delta(T)/2k_BT] \propto 1/R_N$ (R_N is the normal resistance of the junction). The above relations of T_c, E_J and E_C should result in a sharp dependence of T_c on ρ, which was indeed observed in our experiment described above.

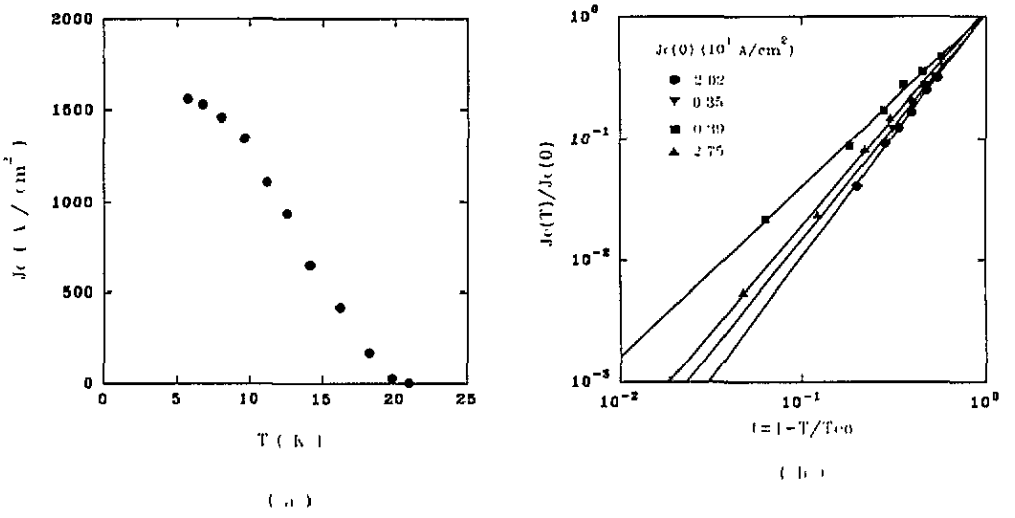

Figure 4. Temperature dependence of the critical current density: (a) $J_c(T)$ curve of the same sample as shown in figure 1; (b) log–log plot of reduced critical current density ($J_c(T)/J_c(0)$) versus the reduced temperature t (= $1-T/T_{c0}$).

The temperature dependence of the critical current density of our Rb_3C_{60} thin-film samples also displays a power-law behaviour near T_c, $J_c(T) = J_c(0)(1 - T/T_c)^\alpha$, as can be seen from figure 4. The power index α is in the range 1.3–2.0. However, both $J_c(0)$ and α have a monotonic dependence on T_c, probably resulting from sample inhomogeneity. In a previous paper [17], Jiang *et al* have proposed an SINS model to interpret the similar $J_c(T)$ behaviour in the weakly linked all-high-T_c edge junctions. If this is the case, we may suppose that I originates from insulating Rb_4C_{60}, Rb_6C_{60} or undoped C_{60} phases, and N from insufficiently diffused Rb metals.

Furthermore, we also measured the voltage–current curves of the Rb_3C_{60} thin films at zero field, as demonstrated in figure 5. At low temperatures, the V–I curves show negative curvature, while at higher temperatures near T_c, the curves exhibit obviously positive curvature. The behaviour is much like that of high-T_c superconductors. In the latter case, Fisher [18] has given a probable explanation in terms of the vortex-glass theory.

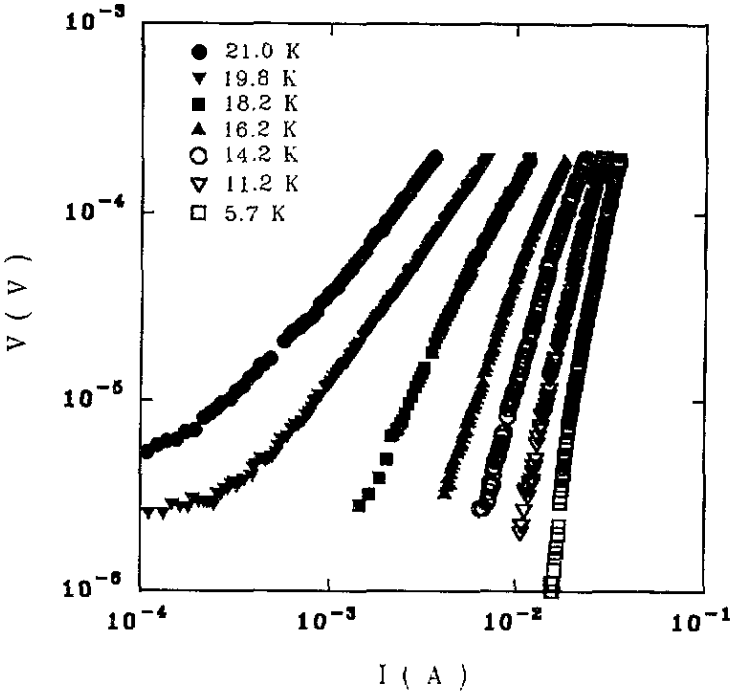

Figure 5. Log–log plot of voltage–current curves.

It is unclear whether we can use the above theory to interpret our experimental results. Further work is now in progress on the Rb fulleride thin films, especially for measurement of the I–V dependence under a magnetic field to explore the more accurate picture of the mixed state in these new type-II superconductors.

In conclusion, we want to emphasize the following main results of our experiments. (1) Superconducting Rb_3C_{60} thin films have been synthesized by doping Rb into epitaxial C_{60} films. The normal-state temperature dependence of the resistivity shows classic metallic behaviour over a wide temperature range from room temperature to 80 K. (2) The high-density intrinsic stacking faults presented in the precursor C_{60} thin films, and hence the low diffusion rate of Rb metals, promoted the formation of non-superconducting phases at disordered {111} closed-packed planes, thus resulting in weak coupling between Rb_3C_{60} superconducting phases. (3) The zero-temperature T_{c0} has a sharp dependence on the sample normal-state resistivity, according to the following empirical formula: $T_{c0} = a + b\rho^{-4.7}$. (4) Near T_c, $J_c(T)$ exhibits power-law behaviour: $J_c(T) = J_c(0)(1 - T/T_c)^{\alpha}$, where α is in the range 1.3–2.0. (5) The dependence of the zero-field current–voltage is similar to that of HTSCs and remains a problem for further research on this new kind of material.

We wish to thank Professor Z Z Gan, R S Han, S Q Feng and Z X Liu for their kind help and useful discussions. This work is supported by the National Centre for Research and Development on Superconductivity and the Graduate Science Foundation of China.

References

[1] Haddon R C *et al* 1991 *Nature* **350** 320

[2] Hebard A F *et al* 1991 *Nature* **350** 600
[3] Rosseinsky M J *et al* 1991 *Phys. Rev. Lett.* **66** 2830
[4] Kelty S P *et al* 1991 *Nature* **352** 223
[5] Fleming R M *et al* 1991 *Nature* **352** 797
[6] Ogata H *et al* 1992 *Japan. J. Appl. Phys.* **31** L166
[7] Xiang X D *et al* 1992 *Science* **256** 1190
[8] Zhao W B *et al* 1993 *Solid State Commun.* **85** 945
[9] Zhao W B *et al* 1993 *Thin Solid Films* at press
[10] Zhao W B *et al* 1993 *Thin Solid Films* submitted
[11] Palstra T T M *et al* 1992 *Phys. Rev. Lett.* **68** 1054
[12] Fisher J E *et al* 1993 *Appl. Phys.* A **56** 193
[13] Crespi V H *et al* 1992 *Phys. Rev.* B **46** 12064
[14] Sparn G *et al* 1992 *Phys. Rev. Lett.* **68** 1228
[15] Fleming R M *et al* 1991 *Nature* **352** 701
[16] Imry Y and Stroking M 1981 *Phys. Rev.* B **24** 6353
[17] Jiang H M *et al* 1993 *Chinese J. Low Temp. Phys.* **15** S293
[18] Fisher M P A 1989 *Phys. Rev. Lett.* **62** 1415